Submitted: 01/16/2026
Accepted: 02/21/2026
Published: 04/10/2026

Research Article

[1] Earth Systems Science, McGill University

Keywords

Boreal peatlands, Net ecosystem exchange, Conservation prioritization, Human footprint

Email Correspondence

sophie.piret@mail.mcgill.ca

https://doi.org/10.26443/msurj.v21i1.412

Piret, Sophie J.[1], Saul, Quinn[1], Châtelier, Simone[1]

Spatial Modeling of Canadian Boreal Peatland Carbon Sinks: An Integrative Framework to Support Climate and Development Policy

Abstract

Peatlands are among the most effective carbon sinks, yet their stability is increasingly threatened by expanding land use and infrastructure. Spatially explicit information remains limited on where Canada's boreal peatlands combine high CO_2 sink strength with low human pressure. We mapped growing-season CO_2 sink potential and identified low-disturbance areas across Canadian boreal peatlands by integrating climate and human footprint data. Using AmeriFlux eddy-covariance data from four Canadian boreal peatland flux-tower sites from 2007–2019, we modeled climatic controls on net ecosystem exchange (NEE) of CO_2 and upscaled predictions with ERA5-Land reanalysis data. A pooled multiple linear regression using air temperature, subsurface soil temperature, and incoming shortwave radiation explained 57% of NEE variance (adjusted R^2=0.57). Comparisons of tower-measured and ERA5-Land climatic variables showed strong agreement for shortwave radiation and modest temperature biases, highlighting uncertainty in regional upscaling. Applying the model across boreal peatlands predicted the strongest sinks in the Northwest Territories and weaker sinks toward the northern boreal margin and mountainous regions. We then derived Predicted Carbon Sink Strength (PCSS) and combined it with an inverted human footprint to construct a Boreal Peatland Conservation Index (BPCI) to prioritize areas with high sink strength and low human footprint. High BPCI values were concentrated in the Hudson Bay Lowlands and the Northwest Territories. Because predictions are based on four flux-tower sites and represent growing-season CO_2 exchange, results are best interpreted as screening-level guidance. Overall, this integrative framework provides an interpretable, updatable approach for identifying boreal peatland regions where protecting CO_2 sinks may deliver high climate benefits with low development conflict.

Introduction

Peatlands are wetlands formed by the accumulation of partially decomposed organic material under water-saturated, low-oxygen conditions. Globally, peatlands cover only ~3% of Earth's land surface yet store ~30% of the world's soil carbon[1, 2]. Total peatland carbon stocks are estimated at 500–600 Pg C, exceeding the carbon stored in the world's forests[2]. Their importance is especially pronounced in Canada, the location of roughly a quarter of the world's peatlands[3], primarily in the boreal region[4], underscoring Canada's role in climate-mitigation planning.

Beyond carbon storage, peatlands support biodiversity, regulate hydrology, improve water quality, and hold cultural significance for many Indigenous communities[1]. Yet affected by drainage, agriculture, peat extraction, mining, and infrastructure development[1, 2]. Drainage increases oxygen exposure and accelerates decomposition, shifting peatlands from long-term carbon sinks toward persistent carbon sources[2]. Wildlife Conservation Society Canada reports that only 13% of Canada's peatlands were protected as of 2023[5], leaving ~87% vulnerable to industrial and land-use pressures. Conservation planning requires maps that extend peatland CO_2 sink estimates beyond the limited network of field sites and place sink potential in the context of human disturbance.

Peatland carbon dynamics are commonly assessed using net ecosystem exchange (NEE), which quantifies the net CO_2 flux between an ecosystem and the atmosphere[6]. NEE reflects the balance between CO_2 uptake through photosynthesis, quantified by gross primary production (GPP), and CO_2 emissions via ecosystem respiration (R)[7, 8]. NEE is commonly expressed as $NEE = R - GPP$, where negative NEE values indicate a net carbon sink, and positive values indicate a net carbon source[9]. Because photosynthesis and respiration are reduced under freezing conditions, peatland CO_2 exchange is most concentrated during the biologically active season[10].

Climate regulates peatland NEE through its effects on photosynthesis and respiration. Air and soil temperatures (TA, TS) affect both processes, with warming often increasing ecosystem respiration and potentially reducing net CO_2 uptake[9, 11]. Incoming shortwave radiation (SWin) provides energy for photosynthesis and is commonly associated with stronger CO_2 uptake during the growing season[7, 9]. Moisture also shapes NEE because saturation suppresses decomposition, whereas drying can increase aerobic respiration and constrain plant productivity. Although water-table depth is a key hydrologic control on peatland carbon exchange[8, 11], it is often challenging to represent at regional scales. This creates an opportunity to use spatially continuous climatic predictors to upscale peatland CO_2 exchange beyond point measurements.

The Canadian Model for Peatlands developed by Bona et al. depends on multiple simplifying assumptions about complex processes such as temperature-sensitive decay and water-table dynamics[11]. This motivates simpler regression-based approaches that leverage widely available climatic variables to predict growing-season NEE. Prior work suggests that wetland NEE can often be captured with relatively simple climate–flux

relationships, motivating regression-based upscaling from AmeriFlux flux-tower observations[9]. While successfully applied in coastal wetlands[7], a comparable regression-based framework to predict and map NEE across boreal Canadian peatlands has not yet been developed. Moreover, the integration of carbon-sink maps with human disturbance metrics remains understudied. This need is especially acute as Canada expands northern access for critical minerals, increasing land-use pressures in regions such as the Hudson Bay Lowlands and the Ring of Fire.

To address this gap, we developed a regression model calibrated with AmeriFlux NEE tower observations and applied it to ERA5-Land climate data to predict NEE across boreal Canada. We used these predictions to construct a Canadian Boreal Peatland Conservation Index (BPCI) to support conservation and climate-mitigation planning. The BPCI integrates predicted NEE with a human footprint index that captures human disturbance from built infrastructure, transportation networks, and land-use conversion[12]. By combining a climate-driven indicator of sink strength with human footprint data, the BPCI highlights regions for further assessment where conservation may maximize CO_2-uptake benefits while prioritizing areas with lower disturbance.

Specifically, we address the following questions:

i) Which widely available climatic predictors are most informative for modeling growing-season NEE at boreal peatland AmeriFlux sites?
ii) How does predicted growing-season NEE vary across boreal Canadian peatlands based on key climatic predictors?
iii) How closely do ERA5-derived climatic predictors match tower-observed values during the growing season? What does this imply for upscaling uncertainty?
iv) Where should conservation be prioritized to maximize predicted CO_2 sink strength while minimizing human disturbance?

Methods

Study area and sites

Our study focuses on the four available boreal Canadian peatland sites in the AmeriFlux eddy-covariance network: the Attawapiskat River Bog (CA-ARB), Attawapiskat River Fen (CA-ARF), Churchill Fen site 1 (CA-CF1), and Scotty Creek Bog (CA-SCB). The combined dataset spans from 2007 to 2019, with individual sites providing varying record lengths. Sites include two bogs and two fens and span latitudes from 52.695°N to 61.308°N. Across sites, mean annual precipitation ranges from 388 to 700 mm, mean annual temperature ranges from −6.5 to −1.3 °C, and elevations range from 16.5 to 280 m (Table 1).

Global Lakes and Wetlands Database v2 (GLWD v2) provides percent coverage per grid cell for 33 wetland and waterbody types from 1990–2020 at 15 arc-seconds (~500 m) resolution. The broader study area of Canadian boreal peatlands was derived from the GLWD v2 by extracting the Arctic/Boreal peatland classes, both forested and unforested[13]. We then constrained the layer to the Canadian boreal extent in ArcGIS Pro to avoid conflating peatlands with different climatic regimes and ecological controls[14]. This produced a boreal peatland extent and fractional-cover layer used for spatial upscaling and index calculations.

Datasets and climate predictors

AmeriFlux is a network of sites that measures ecosystem-atmosphere fluxes using eddy-covariance (EC) towers, along with associated meteorological variables[15]. We used AmeriFlux NEE and meteorological products processed with standard EC corrections and quality control, including low-turbulence filtering and marginal distribution sampling (MDS) gap-filling[16, 17]. GPP and ecosystem respiration are then partitioned from NEE using established flux-partitioning algorithms[16, 18].

ERA5-Land is a global, hourly reanalysis dataset at a resolution of 0.1° (~9 km) produced using a blend of observations and physics-based weather models[19].

We used the 2020 Global 100 m Terrestrial Human Footprint (HFP-100) dataset, which provides global maps of human pressure to quantify anthropogenic disturbance across the study region[12].

We initially considered climate variables shared between AmeriFlux and ERA5-Land based on previous studies[9, 20]. Predictors included 2 m air temperature (TA; °C), soil temperature (TS; °C), incoming shortwave radiation (SWin; W m^2), incoming longwave radiation (LWin; W m^2), and precipitation (P; mm).

Preprocessing and growing-season definition

We standardized AmeriFlux missing values and screened candidate predictors for collinearity prior to regression. Predictor screening based on pairwise Spearman correlations and variance inflation factor (VIF) diagnostics is described in Supplementary Materials (Figure S2). Based on this screening, we retained TA, TS, and SWin for regression and excluded LWin due to strong collinearity with TA.

AmeriFlux soil temperature was harmonized to the ERA5-Land 28–100 cm layer (layer 3) to support consistent upscaling. Details on sensor-depth handling are provided in Supplementary Materials.

To focus on biologically relevant periods, months with mean monthly TA<0°C were excluded from analysis. The rule was applied consistently to tower observations and ERA5-Land predictors. This ensured datasets reflected only the growing season, focusing the analysis on months when CO_2 flux magnitudes are highest in these systems (Supplementary Figure S1). ERA5-Land variables were converted to monthly mean values and AmeriFlux units before agreement testing, growing-season definition, and upscaling. All subsequent analyses used the pooled AmeriFlux dataset.

Exploratory analysis and AmeriFlux regression

We used monthly mean NEE (μmol CO_2 m^{-2} s^{-1}; negative values indicate net CO_2 uptake) as the response variable. We analyzed monthly means to align temporal scale across sites and ERA5-Land, reduce short-term noise and gap-filling artifacts, and focus on seasonal-scale controls suitable for regional screening. To explore broad relationships between climatic variables and NEE, and to inform predictor selection, we computed monthly Spearman's rank correlation coefficients (ρ) between each climatic predictor and NEE (α=0.05), a rank-based measure robust to non-normality and outliers[21]. We also visually assessed scatterplots between NEE and climatic variables to examine linearity, variance structure, and cross-site consistency prior to modeling (Figure 2). Climatic variables included TA, TS, SWin, and log-transformed precipitation (log(P+1)) as a proxy for moisture conditions, noting that precipitation does not fully represent water-table dynamics. Precipitation showed no significant association with NEE in the correlation analysis and was therefore not retained in the final regression model; see results for further discussion of variable selection.

Multiple linear regression was implemented using ordinary least squares to quantify the effects of selected climatic variables on NEE. The final regression for spatial upscaling used TA, TS, and SWin. Regression coefficients were evaluated at α=0.05, and model performance was assessed using

adjusted R^2 and root mean square error.

ERA5-Land agreement and spatial upscaling

We evaluated agreement between tower observations and their equivalent ERA5-Land predictors to assess potential reanalysis biases relevant to NEE upscaling[19]. Predictors included TA, TS, and SWin. The agreement metric and complete results are provided in Supplementary Materials.

The regression model developed from the combined tower data was applied to ERA5-Land reanalysis data to estimate monthly NEE across boreal Canadian peatlands. Predicted NEE was subsequently averaged over time to obtain a single mean growing-season value per pixel.

Conservation index construction

To align rasters, all datasets were projected to a common coordinate system (WGS 1984), clipped to the boreal peatland extent, and resampled to the GLWD v2 grid to enable pixel-wise calculations in ArcGIS. This does not add spatial detail to predicted NEE, because all GLWD pixels within a given ERA5 cell share the same predicted NEE rate per m². Accordingly, predicted NEE and derived indices should be interpreted at the ERA5-Land resolution. All final map outputs were reprojected to the Canada Lambert Conformal Conic projection for presentation.

The Predicted Carbon Sink Strength (PCSS) represents the predicted strength of CO_2 sinks (NEE<0) across boreal peatlands, scaled by the GLWD v2 peatland fractional coverage. To compute PCSS, we multiplied predicted NEE by the peatland fraction within each pixel. To prioritize strong CO_2 sinks, we set positive NEE values to zero before calculating PCSS, thereby excluding carbon-source pixels. The resulting layer was then multiplied by -1 to make sink strength positive, and min–max normalization was applied (Equation 2):

Equation 2:

$$PCSS_{norm} = \frac{PCSS - \min(PCSS)}{\max(PCSS) - \min(PCSS)} \cdot 100$$

The Inverted Human Footprint (IHFP) visualizes human pressure across peatlands within our study area. We used the 2020 Global Terrestrial Human Footprint dataset (HFP-100)[12], which maps the intensity of human pressure at ~100 m resolution. HFP-100 is a composite index of anthropogenic pressure derived from multiple infrastructure, land-use, and population-related indicators.

To quantify human pressure for conservation prioritization, all Canadian tiles were extracted and mosaicked to produce a single seamless raster. To ensure that highly remote pixels received the greatest values, the raster was inverted. The resulting IHFP layer was then normalized using min–max scaling (Equation 3):

Equation 3:

$$IHFP_{norm} = \frac{IHFP - \min(IHFP)}{\max(IHFP) - \min(IHFP)} \cdot 100$$

The BPCI was produced by combining IHFP and PCSS using a weighted scheme (Equation 4). We selected weights through sensitivity testing to balance predicted sink strength with low disturbance, with slightly higher weight on IHFP to retain visibility of human-pressure gradients.

Equation 4:

$$BPCI = 0.6 \cdot IHFP_{norm} + 0.4 \cdot PCSS_{norm}$$

Results

Peatland coverage and site characteristics

Figure 1 shows the boreal peatland extent, fractional peatland cover, and the four AmeriFlux sites. Peatland cover is most contiguous in the Hudson Bay Lowlands, with additional high-cover regions in parts of the Northwest Territories; fractional cover is lower in mountainous regions and across much of eastern boreal Canada.

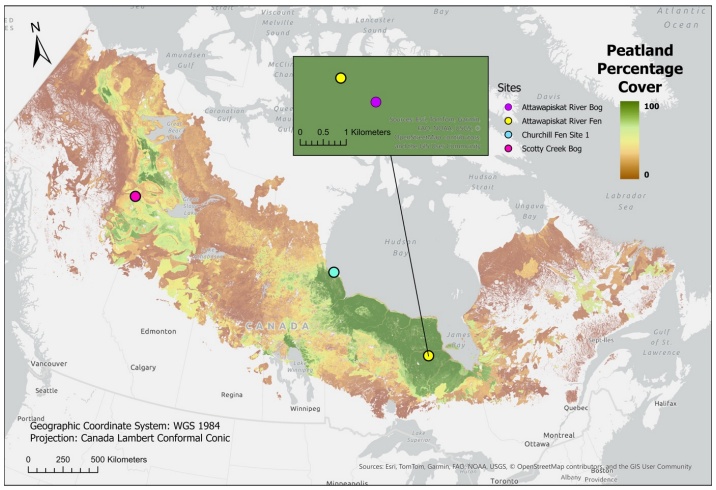

Figure 1. Study area, boreal peatland extent, and flux-tower sites. Map of the Canadian boreal domain showing boreal peatland fractional cover13, the boreal extent14, and four AmeriFlux eddy-covariance sites (CA-ARB, CA-ARF, CA-CF1, CA-SCB)15. The green inset enlarges the Attawapiskat River area in the Hudson Bay Lowlands to distinguish the two closely spaced sites, CA-ARB and CA-ARF; the inset scale bar indicates local distance. Map shown in the Canada Lambert Conformal Conic projection.

Exploratory analysis of climatic predictors

Pairwise correlations among candidate predictors were assessed to screen for collinearity. TA and LWin were strongly correlated (ρ=0.92), exceeding the a priori threshold (|ρ|>0.8). We excluded LWin from subsequent analysis and regression modeling and retained TA as the more interpretable predictor. Multivariable collinearity among the remaining predictors was low (all VIFs<5), supporting their inclusion in candidate models (Supplementary Figure S2). VIF values for the final predictor set were 4.98 for TA, 2.99 for subsurface TS, and 3.25 for SWin.

Using pooled growing-season data, we examined correlations between NEE and the retained predictors TA, TS, P, and SWin (Figure 2). TA (Figure 2A) and TS (Figure 2C) were negatively correlated, with NEE becoming more negative as temperatures increased. The association was stronger for TA than TS (ρ=−0.79 versus ρ=−0.39). The relationship between SWin and NEE was also negative (Figure 2D, ρ=−0.59). Precipitation (log-transformed; Figure 2B) showed no evidence of a significant association with NEE.

Name	Attawapiskat River Bog	Attawapiskat River Fen	Churchill Fen Site 1	Scotty Creek Bog
Site ID	CA-ARB	CA-ARF	CA-CF1	CA-SCB
Wetland Type	Bog	Fen	Fen	Bog
Biome Classification	Boreal	Boreal	Boreal	Boreal
Permafrost Influence	Discontinuous	Discontinuous	Continuous	Discontinuous
Forest Influence	Partially Forested	Partially Forested	Unforested	Unforested
Mean Monthly Precipitation [mm]	700	700	452	388
Mean Monthly Temperature [°C]	-1.3	-1.3	-6.5	-2.8
Elevation [m]	90	88	16.5	280
Start Year of Measurements	2011	2011	2007	2014
End Year of Measurements	2015	2015	2008	2019
Latitude	52.70	52.70	58.67	61.31
Longitude	83.96	83.96	93.83	121.30

Table 1. Summary of the four Canadian boreal peatland AmeriFlux site characteristics and data coverage.

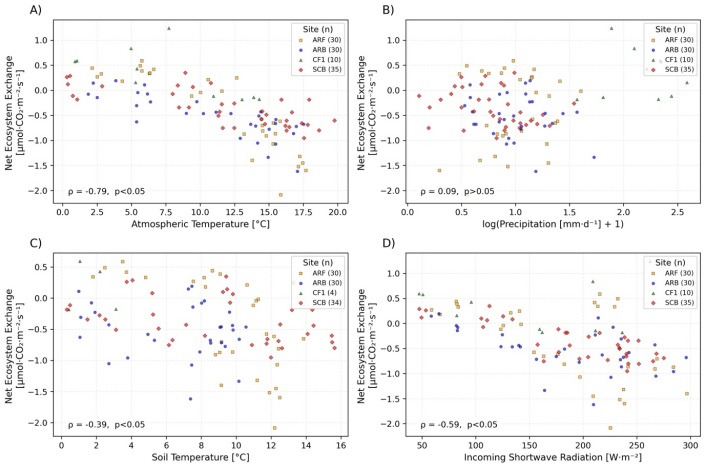

Figure 2. Net ecosystem exchange in relation to climatic predictors across sites during the growing season (TA>0 °C), using pooled monthly data from four AmeriFlux boreal peatland sites. Points are coloured by site. Negative NEE indicates net CO_2 uptake.

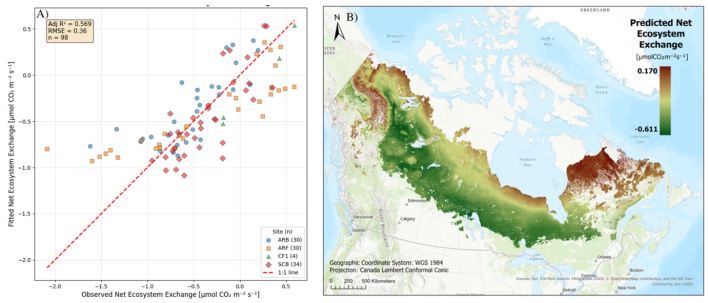

Figure 3. Regression model performance and regional upscaling of growing-season NEE. (A) Observed versus predicted monthly NEE from the pooled multiple linear regression (n=98; adjusted R^2=0.57; RMSE=0.36 μmol CO_2 m^{-2} s^{-1}) using data from four boreal peatland AmeriFlux sites (CA-ARB, CA-ARF, CA-CF1, CA-SCB). (B) Spatially upscaled mean NEE (μmol CO_2 $m^{-2}s^{-1}$) predicted by applying the fitted model to ERA5-Land predictors across boreal Canadian peatlands. Negative values indicate net CO_2 uptake.

The AmeriFlux observations were used to fit a pooled multiple linear regression model to quantify the effects of the selected climatic predictors on growing-season NEE. The final regression used for spatial upscaling with ERA5-Land reanalysis data retained TA, TS, and SWin.

The fitted NEE regression model

Equation 5:

$$NEE_{pred} = 0.7160 - 0.0536 \cdot TA - 0.0023 \cdot SWin - 0.0124 \cdot TS$$

When fit to a pooled growing-season dataset of 98 monthly observations, the model explained 57% of the variability in NEE (adjusted R^2=0.57) and had an RMSE of 0.36 μmol CO_2 $m^{-2}s^{-1}$ (Figure 3A). Among the variables included, TA (β=−0.0536, p=0.001) and SWin (β=−0.0023, p=0.025) were significant predictors, whereas TS was not (β=−0.0124, p=0.423).

The predicted multi-year mean growing-season NEE ranged from −0.611 to 0.170 μmol CO_2 $m^{-2}s^{-1}$ across boreal peatlands (mean=−0.305; SD=0.120). The strongest sinks occur in the interior, particularly in the Northwest Territories, with sink strength weakening toward the northern boreal margin and mountainous/northeastern regions (Figure 3B).

We next assessed agreement between tower-observed and ERA5-Land predictors using percent differences (Figure 4). SWin showed the strongest agreement, whereas TA and TS exhibited modest, seasonally varying biases that were most pronounced in shoulder months. Full agreement results are shown in Supplementary Materials.

Boreal Peatland Conservation Index and component layers

A map of normalized PCSS, with higher values indicating higher predicted sink strength, is depicted in Figure 5A. PCSS scales predicted NEE by peatland fractional cover and exhibits pronounced regional variation (mean=18.84; *SD*=17.89). High PCSS values are concentrated in the central Hudson Bay Lowlands and parts of northern Manitoba and the Northwest Territories, particularly between Great Bear Lake and Great Slave Lake. By contrast, eastern regions, including northern Quebec and Labrador and mountainous areas, show lower PCSS values, with many pixels near zero. Figure 5B maps IHFP, with higher values indicating lower human pressure. IHFP is broadly high across peatland regions, reflecting generally low human pressure overall (mean=99.30; *SD*=2.59), with localized low-IHFP corridors and nodes concentrated along the southern boreal margin. These features align with major transportation routes, settlement clusters, and resource-extraction areas, where development pressure is pronounced.

Finally, Figure 5C shows BPCI values across Canadian boreal peatlands, with higher values indicating higher PCSS and lower human footprint. The largest contiguous areas of high BPCI values occur across the southern Hudson Bay Lowlands. High BPCI values also appear in the Northwest Territories, between Great Bear Lake and Great Slave Lake, and north of Lake Winnipeg. Low BPCI occurs along the southern margin, near corridors/settlements, and across much of eastern boreal Canada.

Discussion

This study develops a climate-driven regression model that upscales growing-season peatland NEE and combines an IHFP layer with predicted CO_2 sink potential to produce a conservation index. By linking tower-derived relationships to ERA5-Land predictors, the workflow produces interpretable first-pass maps to support conservation and land-

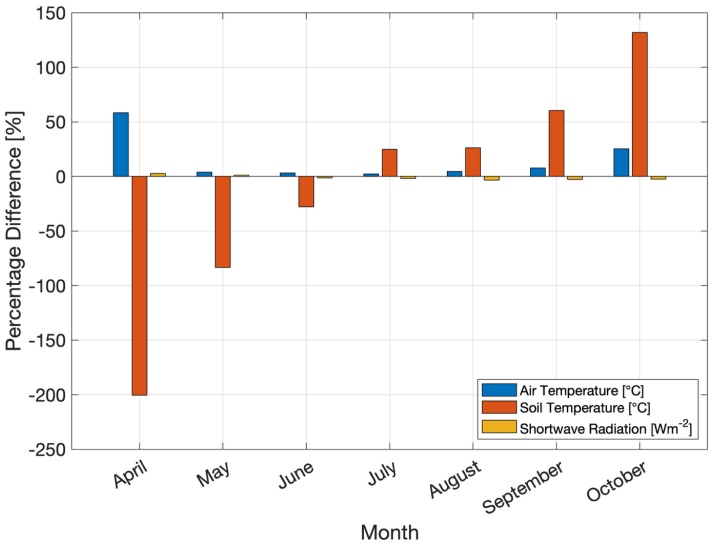

Figure 4. Agreement between tower-observed and ERA5-Land predictors during the growing season (TA>0 °C). Percent difference between ERA5-Land and tower-observed monthly growing-season predictors (TA, TS, SWin) at the four study sites. Positive values indicate ERA5-Land exceeds tower observations; negative values indicate underestimation.

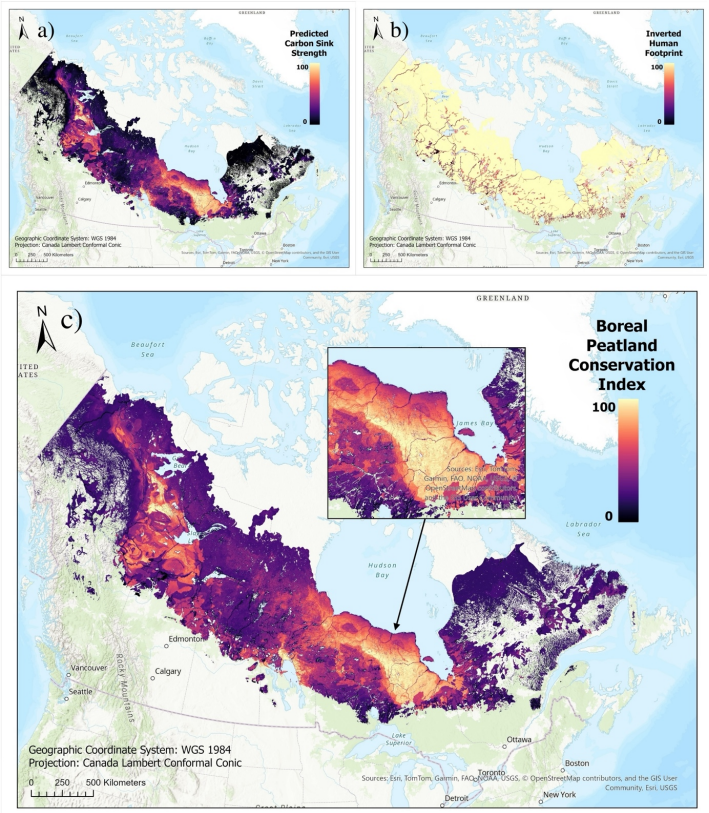

Figure 5. Boreal Peatland Conservation Index and component layers. (A) Predicted carbon sink strength (PCSS), derived from predicted NEE after setting source pixels (NEE>0) to zero, scaling by peatland fractional cover, and applying min–max normalization. (B) Inverted human footprint (IHFP), derived by inverting human footprint values and applying min–max normalization so that higher values indicate lower human pressure. (C) Boreal Peatland Conservation Index, calculated as a weighted combination of normalized IHFP and normalized PCSS.

use planning. This empirical approach offers a transparent complement to process-based national peatland frameworks[11]. The model explained 57% of monthly growing-season NEE variance, supporting its use for first-pass prioritization. While these maps are intended to help target consultation and research, conservation decisions should incorporate field validation, land tenure, Indigenous governance and knowledge, local governments, and current and proposed development.

Climatic controls on growing-season NEE

Across observations, NEE was negatively correlated with TA and SWin, with a weaker but significant negative association with TS, reflecting stronger net CO_2 uptake during warmer, brighter months. Similarly, SWin captures an energy-availability signal in line with radiation controls on photosynthesis. Precipitation was not significantly associated with NEE and was therefore not retained for multivariable modeling.

In the multivariable model, TA and SWin best explained growing-season NEE and remained significant predictors, indicating that temperature and radiation capture much of the predictable variability, as in other regional NEE upscaling studies[7,8]. TS, while negatively correlated with NEE in pairwise analyses, was not significant in the multivariable model, likely because subsurface TS is less directly linked to near-surface fluxes and shares seasonality with other predictors. However, excluding TS reduced adjusted R^2, suggesting a modest complementary contribution and supporting its inclusion in the model.

Although TA and TS remained moderately correlated because of shared seasonal structure, VIF values indicated that multivariable redundancy in the retained predictor set remained within acceptable limits.

Upscaling assumes these climate-NEE relationships transfer across boreal peatlands. Figure 2 supports a first-order pooled model, but predictions are most reliable within tower-observed predictor ranges and become less certain under extrapolation. Given that adjacent CA-ARF/CA-ARB towers contribute a large share of the observations (61%), the fitted relationships may be weighted toward conditions at these sites, underscoring the value of expanding flux coverage across the boreal region.

Calibrated on four AmeriFlux peatland sites spanning bog and fen systems across discontinuous to continuous permafrost settings, the model represents only the conditions sampled by these towers. In particular, the calibration dataset does not explicitly capture gradients in nutrient status, vegetation structure (open, treed, or forested systems), or the diversity of permafrost–hydrologic regimes present across the boreal region. Process-based national modeling indicates that peatland CO_2 exchange varies across these ecosystem classes, with typically stronger uptake associated with forested peatlands and nutrient-rich fen systems[11]. Regional climatic gradients may also influence the transferability of climate–NEE relationships. For example, differences in moisture balance between western and eastern boreal regions can affect peatland productivity and respiration dynamics[11]. Consequently, the pooled regression approach captures first-order climatic controls on NEE but may not fully represent ecological and regional variability across all Canadian boreal peatlands.

Reanalysis agreement and uncertainty

Tower-reanalysis comparisons show good agreement for TA and SWin during core growing-season months. Agreement weakens for TA in shoulder months, and TS shows larger, more seasonally variable percent differences. Because tower temperatures can approach 0 °C in shoulder months, small denominators can inflate percent differences, so temperature-based percent differences should be interpreted cautiously. Given the coarse ERA5-Land grid (~9 km) relative to tower footprints and sub-pixel heterogeneity

in peatlands and climate, our maps are best interpreted for regional screening rather than pixel-scale flux estimates; additional detail is provided in Supplementary Materials.

Spatial patterns in sink potential

With these uncertainties in mind, the upscaled maps show clear regional structure in sink strength. Predicted NEE and PCSS indicate strong sink potential in the southern Hudson Bay Lowlands and parts of northern Manitoba and the Northwest Territories, weakening toward mountainous or low-cover regions and the northern margin, likely reflecting lower temperatures and reduced energy availability at higher latitudes. Weighting by peatland fractional cover highlights high-cover regions but introduces uncertainty associated with wetland classification[13]. In addition, data alignment and resampling choices can smooth local extremes, and our sink-focused PCSS approach sets positive NEE to zero, omitting information on predicted CO_2 sources.

Broad spatial patterns in our NEE predictions are consistent with national peatland simulations from the Canadian Model for Peatlands (CaMP)[11]. Although CaMP is process-based, both analyses highlight the Hudson Bay Lowlands as major peatland sink regions and indicate comparatively weaker sink signals across eastern boreal Canada and mountainous areas[11]. We interpret this agreement as convergence in regional patterns that supports the use of our maps for preliminary conservation screening.

Conservation prioritization and feasibility

The BPCI combines PCSS with human footprint to highlight areas with strong predicted sinks and low disturbance. These priority areas cluster in the southern Hudson Bay Lowlands, with additional hotspots in the Northwest Territories and northern Manitoba. The BPCI can help flag areas where protecting strong carbon sinks may warrant assessment of conservation opportunities and potential project impacts. The high-scoring area in the southern Hudson Bay Lowlands appears largely spatially separated from the Ring of Fire mines and, apart from the Victor Diamond Mine, occurs in highly remote areas, which may increase the feasibility of proactive protection[22]. However, because this region overlaps with Indigenous communities[22], BPCI should be treated as a screening input for partnership-led planning and validation rather than a standalone prescription. By contrast, the northern Manitoba hotspot overlaps more strongly with existing human pressure, implying greater conflict and lower near-term feasibility than similarly strong sinks in lower-pressure areas.

Limitations and future directions

Key considerations include sparse flux coverage and limited representation of hydrologic controls that strongly regulate peatland respiration and productivity[23]. CO_2 emissions can continue during the non-growing season and may offset part of the growing-season uptake[24]. Accordingly, our results represent growing-season CO_2 sink potential rather than the annual net carbon balance. Additionally, NEE describes ecosystem-atmosphere CO_2 exchange but is missing disturbance losses such as wildfire. Process-based peatland modeling indicates that wildfire can substantially negate long-term carbon sinks when moving from ecosystem productivity metrics to net biome productivity[11]. Given the importance of water-table depth for peatland CO_2 exchange and its coupling to CH_4 dynamics[10, 23, 25], future work should test spatial hydrology proxies such as drought code indices or remotely sensed soil moisture products[26]. As a multiple linear regression, the approach may under-represent non-linear or threshold responses in climate-NEE relationships. AmeriFlux gap-filling improves completeness but can introduce additional uncertainty, especially where data gaps are long. Subsurface soil-temperature harmonization may also introduce uncertainty because tower sensor depths vary across sites and do not perfectly match ERA5-Land layers. Monthly aggregation and time averaging supports regional comparability but can smooth short-lived climatic extremes that affect CO_2 exchange. Because agreement was assessed using percent differences, which can be inflated near 0 °C, reporting absolute bias alongside percent differences would further clarify agreement patterns. Bias-correcting ERA5 meteorological inputs to better match tower-observed climate variables, along with sensitivity analyses to quantify how ERA5 biases propagate into NEE predictions, would help bound uncertainty in flux estimates. Additional flux sites, longer time series, and annual carbon-balance estimates would increase representativeness and confidence in extrapolation. Because our calibration period spans 2007–2019, future work should incorporate newer observations as climate conditions evolve; extending the framework to include climate projections could help evaluate the persistence of current sink hotspots under a warming climate. Model evaluation would also benefit from leave-one-site-out cross-validation as additional sites become available.

Regarding disturbance and implementation feasibility, HFP-100 may under-represent fine-scale or rapidly changing disturbances, including emerging resource extraction sites. Because CO_2-only prioritization can misrepresent net climate benefits in methane-rich systems[2], future work should integrate CH_4 alongside CO_2-based NEE. Alternative weightings and additional data layers could be incorporated to reflect different policy goals while maintaining the workflow. Adding wildfire risk, permafrost vulnerability, and proximity to planned development could better target lasting climate benefits.

Conclusion

Taken together, this study offers a framework for identifying boreal peatland regions where protecting CO_2 sinks could yield substantial climate benefits with minimal development conflict. The generated maps indicate strong CO_2 uptake in parts of the Northwest Territories and, after accounting for peatland fractional cover, highlight potential high-priority areas within extensive peatland complexes, including the southern Hudson Bay Lowlands. By combining sink strength with low human pressure, the Conservation Index offers a practical screening tool to support targeted field validation, consultation, and further modeling. Future extensions that incorporate CH_4 fluxes, hydrologic controls, permafrost dynamics, and more recent data will improve estimates of net climate benefits as climate and land-use pressures evolve.

Acknowledgements

This research was made possible through the guidance, mentorship, and encouragement of Dr. Geneviève Ali and Dr. Peter Douglas.

Supplementary Materials

Supplementary material referenced in the text of this article may be found online at https://doi.org/10.26443/msurj.v21i1.412.

References

1. Goodday, V., Harris, L. & Tanguay, L. *Assessing Peatland Law and Policy Across Canada: Is Canada Fulfilling Its Critical Stewardship Role?* (Wildlife Conservation Society Canada, 2024).

2. Charman, D. J. in *Encyclopedia of Inland Waters* (eds Likens, G. E.) 541–548 (Academic Press, 2009).

3. Harris, L. I. et al. The essential carbon service provided by northern peatlands. *Frontiers in Ecology and the Environment* **20,** 222–230 (2022). 10.1002/fee.2437

4. Tarnocai, C. The effect of climate change on carbon in Canadian peatlands. *Global and Planetary Change* **53,** 222–232 (2006). 10.1016/j.gloplacha.2006.03.012

5. Wildlife Conservation Society Canada. *Canadian policy failures putting globally important carbon-rich peatland ecosystems at risk, says new report* 2024. https://wcscanada.org/newsroom/news/canadian-policy-failures-putting-globally-important-carbon-rich-peatland-ecosystems-at-risk-says-new-report/.

6. Reichle, D. E. in *The Global Carbon Cycle and Climate Change* (eds) 119–156 (Elsevier, 2020).

7. Lu, Y., Huang, Y., Jia, Q. & Xie, Y. Capturing the net ecosystem CO2 exchange dynamics of tidal wetlands with high spatiotemporal resolution by integrating process-based and machine learning estimations. *Agricultural and Forest Meteorology* **352,** 110045 (2024). 10.1016/j.agrformet.2024.110045

8. Fei, X. et al. Eddy covariance and biometric measurements show that a savanna ecosystem in Southwest China is a carbon sink. *Scientific Reports* **7,** 41025 (2017). 10.1038/srep41025

9. Wood, D. A. Net ecosystem exchange comparative analysis of the relative influence of recorded variables in well monitored ecosystems. *Ecological Complexity* **50,** 100998 (2022). 10.1016/j.ecocom.2022.100998

10. Strachan, I. B., Pelletier, L. & Bonneville, M.-C. Inter-annual variability in water table depth controls net ecosystem carbon dioxide exchange in a boreal bog. *Biogeochemistry* **127,** 99–111 (2016). 10.1007/s10533-015-0170-8

11. Bona, K. A. et al. Using the Canadian Model for Peatlands (CaMP) to examine greenhouse gas emissions and carbon sink strength in Canada's boreal and temperate peatlands. *Ecological Modelling* **490,** 110633 (2024). 10.1016/j.ecolmodel.2024.110633

12. Mazzariello, J. & Gassert, F. *Global 100m Terrestrial Human Footprint (HFP-100)* (Dryad, 2023).

13. Lehner, B. et al. Mapping the world's inland surface waters: an upgrade to the Global Lakes and Wetlands Database (GLWD v2). *Earth System Science Data* **17,** 2277–2329 (2025). 10.5194/essd-17-2277-2025

14. Brandt, J. P. The extent of the North American boreal zone. *Environmental Reviews* **17,** 101–161 (2009). 10.1139/A09-004

15. Chu, H. et al. AmeriFlux BASE data pipeline to support network growth and data sharing. *Scientific Data* **10,** 614 (2023). 10.1038/s41597-023-02531-2

16. Reichstein, M. et al. On the separation of net ecosystem exchange into assimilation and ecosystem respiration: review and improved algorithm. *Global Change Biology* **11,** 1424–1439 (2005). 10.1111/j.1365-2486.2005.001002.x

17. Pastorello, G. et al. The FLUXNET2015 dataset and the ONEFlux processing pipeline for eddy covariance data. *Scientific Data* **7,** 225 (2020). 10.1038/s41597-020-0534-3

18. Lasslop, G. et al. Separation of net ecosystem exchange into assimilation and respiration using a light response curve approach: critical issues and global evaluation. *Global Change Biology* **16,** 187–208 (2010). 10.1111/j.1365-2486.2009.02041.x

19. Hersbach, H. et al. The ERA5 global reanalysis. *Quarterly Journal of the Royal Meteorological Society* **146,** 1999–2049 (2020). 10.1002/qj.3803

20. Li, M. et al. Key Environmental and Ecological Variables of Wetland CH4 and CO2 Fluxes Change With Warming. *Earth's Future* **13,** e2024EF005751 (2025). 10.1029/2024EF005751

21. Petzoldt, T. *Data Analysis with R: Selected Topics and Examples* 2020. https://wwwpub.zih.tu-dresden.de/~petzoldt/elements_en.pdf.

22. Gamble, J. *What's at stake in Ontario's Ring of Fire* 2017. https://canadiangeographic.ca/articles/whats-at-stake-in-ontarios-ring-of-fire/.

23. Lafleur, P. M., Roulet, N. T., Bubier, J. L., Frolking, S. & Moore, T. R. Interannual variability in the peatland-atmosphere carbon dioxide exchange at an ombrotrophic bog. *Global Biogeochemical Cycles* **17,** 1036 (2003). 10.1029/2002GB001983

24. Rafat, A. et al. Non-growing season carbon emissions in a northern peatland are projected to increase under global warming. *Communications Earth and Environment* **2,** 1–10 (2021). 10.1038/s43247-021-00184-w

25. Strack, M. & Waddington, J. M. Response of peatland carbon dioxide and methane fluxes to a water table drawdown experiment. *Global Biogeochemical Cycles* **21,** GB1007 (2007). 10.1029/2006GB002715

26. Copernicus Climate Change Service. *Fire danger indices historical data from the Copernicus Emergency Management Service* 2019.